Validation of a NTM model using databases of disruptive plasmas at JET

G. Miron[1] and JET Contributors*

[1] *National Institute for Lasers, Plasma and Radiation Physics, Magurele-Bucharest, Romania*

* *See the author list of "Overview of JET results for optimising ITER operation" by J. Mailloux et al. to be published in Nuclear Fusion Special issue: Overview and Summary Papers from the 28th Fusion Energy Conference (Nice, France, 10-15 May 2021)*

Model description

In order to obtain an explicitly derived dynamic form for the perturbed NTM flux function, the associated perturbed equations have to be solved in the whole space [1, 2, 3]. The final form of the perturbed ideal plasma momentum equations is derived for a 3D approach involving natural coordinates (r, θ, φ) and plasma shaping parameters, within the low inverse aspect ratio approximation

$$\sum_{p=0}^{4}\sum_{l=p}^{4}\binom{l}{p}\sum_{\alpha=\max(l,2)-2}^{\min(l,2)}\sum_{j,k}(-\mathrm{i}k\Omega_z)^{l-p}\left[\left(D^{\xi}_{Zl-\alpha}D^{\Phi}_{N\alpha}-D^{\xi}_{Nl-\alpha}D^{\Phi}_{Z\alpha}\right)\frac{\partial^p\Phi^{jk}}{\partial t^p}\right. \tag{1}$$
$$\left.+\left(D^{\xi}_{Zl-\alpha}D^{\Phi'}_{N\alpha}-D^{\xi}_{Nl-\alpha}D^{\Phi'}_{Z\alpha}\right)\frac{\partial^p\Phi'^{jk}}{\partial t^p}\right]\exp[\mathrm{i}(j\theta-k\varphi)]=0$$

The parametrization of the perturbed magnetic field as $\mathbf{b}=\nabla\times\left\{\left[(1/B)\nabla\Phi\times\hat{\mathbf{n}}+\xi_{||}\hat{\mathbf{n}}\right]\times\mathbf{B}\right\}$ has been used by means of Φ and the parallel displacement to the equilibrium magnetic field $\xi_{||}$, where $\hat{\mathbf{n}}=\mathbf{B}/B$. j, k are the poloidal and toroidal number associated with the perturbed quantities Fourier expansion, Ω_z is the plasma toroidal angular rotation frequency and the D quantities stand for various mixed spatio-temporal differential operators applied to the perturbation. For a plasma surrounded by a set of in-vessel rectangular saddle coils consisting of an upper and a lower set of coils on both sides of the median plane the obtained circuit equations are

$$\chi^{mn}_{f+}-\chi^{mn}_{f-}=\lambda_{mn}\sum_{j,k}\frac{1}{k}\left(B^{jkmn}_{1sff}\frac{\partial\chi^{jk}_{s+}}{\partial t}+B^{jkmn}_{2sff}\frac{\partial\chi^{jk}_{f-}}{\partial t}\right) \tag{2}$$
$$+\frac{\lambda_{mn}R}{4R_0}\sum_{p=1}^{2}\sum_{q=1}^{N}\left\{I^{DC}_{pq}[(2-p)\cos\Delta\varphi+p-1]+I^{AC}_{pq}\exp(-\mathrm{i}\Omega_{MP}t)\right\}\exp[-\mathrm{i}(m\theta_p-n\varphi_q)]$$

$\mathbf{b}=\nabla\chi$ and a B-type coils [4] has been chosen to be considered for the sake of calculus simplicity, each coil carrying a static I^{DC}_{pq} and rotational I^{AC}_{pq} signal, the latter at the rotational frequency Ω_{MP}. Each coil is centered at a (θ_p, φ_q) coordinate. The toroidal phase difference between the upper and lower rows of coils is $\Delta\varphi$. $\chi^{mn}_{f\pm}$ and χ^{mn}_{s+} are the perturbed flux function on both coil sides and on the outer side of the magnetic island, respectively. A similar approach is used for a thin, inhomogenously resistive wall, supposed to approximately lie on a magnetic surface

$$\chi_{w+}^{mn} = \chi_{w-}^{mn} + \frac{\mu_0 \delta_w r_w^2 \sigma_w}{m^2} \left\{ \frac{\partial \chi_{w-}^{\prime mn}}{\partial t} + \sum_{h=-3}^{3} \left[I_{1w}^{h} \frac{\partial \chi_{w-}^{\prime m+h,n}}{\partial t} + (m+h) I_{2w}^{h} \frac{\partial \chi_{w-}^{m+h,n}}{\partial t} \right] \right\} \tag{3}$$

$\chi_{w\pm}^{mn}$ is the perturbed flux function on both sides of the wall. δ_w r_w and σ_w are the wall thickness, radial position and conductivity whereas the I quantities are exactly derived expressions of wall radial position. The perturbed vacuum equations satisfy the equation below in natural coordinates and the solution is searched within the lower inverse aspect ratio development $\varepsilon = a/R_0$

$$\Delta \chi = \frac{1}{\sqrt{g}} \sum_{i,j=1}^{3} \frac{\partial}{\partial u^i} \left(\sqrt{g}\, g^{ij} \frac{\partial \chi}{\partial u^j} \right) = 0, \qquad \chi^{m,n} = \chi^{m,n(0)} + \varepsilon \chi^{m,n(1)} + O(\varepsilon^2) \tag{4}$$

Continuity equations of the perturbed magnetic field across the wall and coils have been derived

$$\chi_{w-}^{mn} = \frac{1}{A_{2fwf}^{m0}} \Big[A_{1sff}^{m0} \chi_{s+}^{mn} + A_{2sff}^{m0} \chi_{f-}^{mn} - A_{1fwf}^{m0} \chi_{f+}^{mn} \tag{5}$$

$$+ \sum_{h=-3}^{3} \left(A_{sffwf}^{22m+h,h} \chi_{s+}^{m+h,n} - A_{sffwf}^{12m+h,h} \chi_{f-}^{m+h,n} + A_{fwfwf}^{12m+h,h} \chi_{f+}^{m+h,n} \right) \Big]$$

$$\chi_{w+}^{mn} = \frac{1}{A_{2w\infty w}^{m0}} \left[A_{1fww}^{m0} \chi_{f+}^{mn} + A_{2fww}^{m0} \chi_{w-}^{mn} + \sum_{h=-3}^{3} \left(A_{fw\infty}^{1m+h,h} \chi_{f+}^{m+h,n} + A_{fw\infty}^{2m+h,h} \chi_{w-}^{m+h,n} \right) \right] \tag{6}$$

The A quantities are exactly derived terms of island, coils and wall radial positions. It can be observed that, as in the wall case, the plasma shaping parameters couple the main perturbation with the neighboring ones. Finally the system of the perturbed equations is completed by the boundary perturbed equation across the magnetic island that basically couples the Rutherford equation with the ones mentioned above. The perturbed jump equation across the magnetic island (bootstrap approach) becomes

$$\chi_{s+}^{mn} = \frac{1}{m R_0 q_{s-}} \left\{ \left[m s_{s-} - r_s (n - n q_{s-}) \alpha_m^s \right] \Phi_{s-}^{mn} - r_s (m - n q_{s-}) \left(\alpha_m^{st} \frac{\partial \Phi_{s-}^{mn}}{\partial t} + \Phi_{s-}^{mn'} \right) \right\} \tag{7}$$

q_{s-} and s_{s-} are the safety factor and shear at the level of the inner magnetic island boundary. The heuristic bootstrap term quantity $\alpha_m^s = -a_{BS} \beta_{pol} (L_q/L_p) \sqrt{r_s/R_0} (w/w^2 + w_0^2)$ is used with $\alpha_m^{st} = 8 m \tau_R R_0 / (n r_s^2 s_{s-} B_z w)$. The magnetic island width is chosen as an obvious initial guess $w \cong 2 r_s (m - n q_{s-}) / (m q_{s-} s_{s-})$. All the above equations have finally the general solution

$$\Psi_s^{mn}(t) \cong \frac{\mathrm{i}}{R_0 q_{s-}} (m - n q_{s-}) \Phi_{s-}^{mn} = A_s^{mn} + B_s^{mn} \exp(-\mathrm{i} \Omega_{MP} t) + \sum_{p=1}^{7L} C_{ps}^{mn} \exp(\tau_p t) \tag{8}$$

and a similar solution for the radial derivative, $\Psi_s^{mn'}(t)$. A_s, B_s and C_{ps}^{mn} are exactly derived parametrically quantities, τ_p are the solutions of the Laplace transformed complete system of the perturbed differential equations and $L > 1$ is the number of the considered modes of perturbation. We assume that this is the perturbed magnetic flux function associated to the NTM. This assumption is to be checked against the experimental results during various discharges at JET.

Model testing against JET results

Experimental data at JET is collected in order to be used for the derivation of our modeled calculated results that are finally compared against the interactive plots provided by the JET Mode Analysis MHD python code developed by E. Giovannozzi [5], concerning the modes amplitude, frequency and radial location. We have chosen a number of JET experiments whose dynamic dependencies provided by the JET Mode Analysis code are continuous and robust enough, in order to test our model validity. A too scattered or fragmented experimental plot is more difficult to be followed in order to check whether our calculated dependencies match or not the experimental ones. For a better accuracy the r_s quantity has been taken by using the major radius of the NTM magnetic surface, provided by the same analysis code. It has been used the EFIT equilibrium reconstruction constrained by polarimetry measurements (called EFTF at JET) for the plasma safety factor, shear, pressure, pressure radial derivative, toroidal current density, plasma minor and major radius, poloidal beta and the plasma boundary ellipticity and triangularity. The toroidal plasma rotation and the ions temperature are collected from using

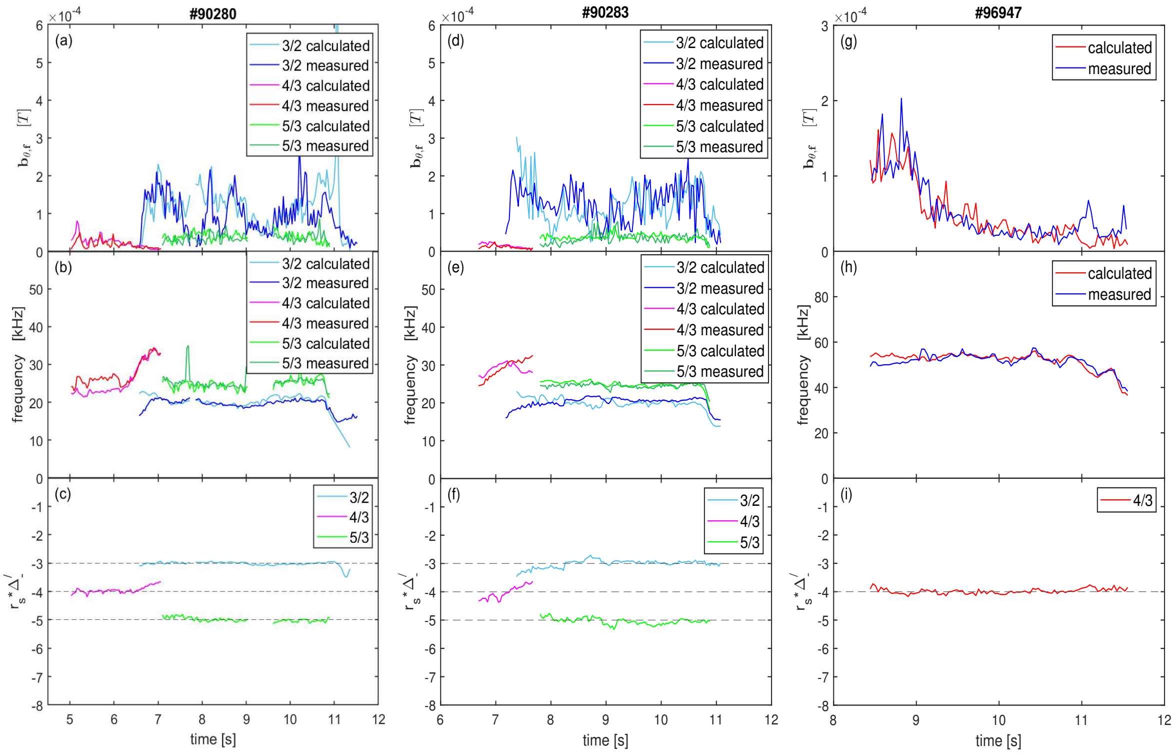

Figure 1: JET 90280, 90283 and 96947 shots measured vs calculated perturbations amplitude ((a),(d),(g)) and frequency ((b),(e),(h)) and the inner term of the calculated stability index ((c),(f),(i))

the charge exchange recombination spectroscopy diagnostics. The High Resolution Thomson Scattering system on JET provides the density and temperature of the electrons via Thomson scattered laser light. Finally the effective ionic charge quantity is collected from spectroscopy diagnostics using Bremmstrahlung signal along the vertical channel in plasma. The pulses are from the hybrid scenario development experiments, described in Ref. [6] and [7]. For the JET pulse no. 90280 figures 1(a) and 1(b) shows a good match between the $3/2$, $4/3$ and $5/3$ NTM modes experimental and calculated amplitudes and frequencies, respectively. The modes amplitude is measured at the JET Fast Magnetic Aquisition System diagnostic coils level in terms of the perturbed poloidal magnetic field. The experimental amplitude is compared to the calculated amplitude $b_{\theta f} \cong 2(r_s/r_f)^{m+1} b_{rs} = 2m(r_s^{m+2}/r_f^{m+1})|\Psi_s^{mn}|$, b_{rs} being the perturbed radial magnetic field at r_s. The mode frequency is calculated as $Im[(\partial\Psi_s^{mn}/\partial t)/\Psi_s^{mn}]$ to be compared to the mode Figure 1(c) shows the inner term of our calculated normalized stability index $r_s\Delta'_{s-} \equiv -r_s Re(\Psi_s^{mn'}/\Psi_s^{mn})$. A closed behavior around the expected $-m$ value has been obtained for every mode. An initial value at the inner magnetic island boundary for $q_{s-} = 1.425$, 1.243 and 1.614 has been chosen for the $3/2$, $4/3$ and $5/3$ modes, respectively. q_{s-} quantity basically provides the initial width of the island. A similar analysis is performed for the JET pulse no. 90283 and for JET 96947 for the $4/3$ mode only. A good match is again retrieved between the calculated and measured quantities in figures 1(d), 1(e), 1(g) and 1(h). $r_s\Delta'_{s-}$ also approximately matches the $-m$ values for all the considered perturbations (see figures 1(f), 1(i)). q_{s-} is chosen as 1.454, 1.223 and 1.614 for the $3/2$, $4/3$ and $5/3$ modes, respectively for the 90283 shot and 1.297 for $4/3$ mode in the 96947 shot case. To conclude, the good match between the perturbation calculated and measured data, also retrieved for these shots, seems to validate the theoretical interpretativemodel we have proposed as long as reliable diagnostic data is provided.

Acknowledgements

This work has been carried out within the framework of the EUROfusion Consortium and has received funding from the Euratom research and training programme 2014-2018 and 2019-2020 under grant agreement number 633053. The views and opinions expressed herein do not necessarily reflect those of the European Commission.

References

[1] R. Fitzpatrick 2009, *Phys. Plasmas* **16** 032502

[2] R. Fitzpatrick and J. Bialek 2006, *Phys. Plasmas* **13**

[3] I.G. Miron 2008, *Plasma Phys. Controlled Fusion* **50** 095003

[4] W. Suttrop et al 2009, *Fusion Eng. and Design* **84** 290

[5] E. Giovannozzi (https://users.euro-fusion.org/openwiki/index.php/MHD-python_code)

[6] C. D. Challis et al, "Impact of neon seeding on fusion performance in JET ILW hybrid plasmas", P2.153, EPS Conference on Plasma Physics, Belfast, Northern Ireland, 26 - 30 June 2017

[7] J. Garcia et al, "Integrated scenario development at JET for DT operation and ITER risk mitigation", 28th IAEA Fusion Energy Conference, 10–15 May 2021